Lawrence Berkeley National Laboratory

Lawrence Berkeley National Laboratory

Title
An analysis of the x-ray linear dichroism spectrum for NiO thin films grown on vicinal Ag(001)

Permalink
https://escholarship.org/uc/item/7z54g8sg

Author
Wu, Y.Z.

Publication Date
2008-09-22

eScholarship.org Powered by the California Digital Library
University of California

An analysis of the x-ray linear dichroism spectrum for NiO thin films grown on vicinal Ag(001)

Y. Z. Wu[1,2], Y. Zhao[3], E. Arenholz[4], A. T. Young[4], and B. Sinkovic[3], Z. Q. Qiu[2],

[1] Surface Physics Laboratory and Department of Physics, Fudan University, Shanghai 200433, P. R. China

[2] Department of Physics, University of California at Berkeley, Berkeley CA 94720

[3] Department of Physics, University of Connecticut, Storrs, CT 06269

[4] Advanced Light Source, Lawrence Berkeley National Lab., Berkeley, CA 94720

Antiferromagnetic (AFM) NiO thin films are grown epitaxially on vicinal Ag(118) substrate and investigated by x-ray linear dichroism (XLD). We find that the NiO AFM spin exhibits an in-plane spin reorientation transition from parallel to perpendicular to the step edges with increasing the NiO film thickness. In addition to the conventional L_2 adsorption edge, x-ray linear dichroism (XLD) effect at the Ni L_3 adsorption edge is also measured and analysized. The result identifies a small energy shift of the L_3 peak. Temperature-dependent measurement confirms that the observed XLD effect in this system at the normal incidence of the x-rays originates entirely from the NiO magnetic ordering.

1. Introduction

Antiferromagnetic thin films have been applied to many forefront spintronics devices because of their characteristic magnetic properties, especially because of the so-called exchange bias effect which shows a unidirectional magnetic anisotropy in a field-cooled antiferromagnet-ferromagnet (AFM-FM) system [1]. Although a complete description of the exchange bias is not yet available, it is believed that the spin structure of the antiferromagnetic (AFM) materials plays an important role [2,3,4]. As compared to the research on FM materials, it remains as an experimental challenge to probe the spin structure of an antiferromagnetic thin film simply because of the zero net spin in an AFM material. This difficulty has been partially overcome recently by the development of the X-ray Magnetic Linear Dichroism (XMLD) technique [5,6]. The XMLD effect probes the local spin axis in an AFM by measuring the absorption coefficient across a core threshold at different polarization angles of a linearly polarized x-ray relative to the sample crystallographic axes [5,6,7,8]. In addition, the XMLD also provides magnetic contrast with chemical and surface sensitivity [9,10,11,12]. By measuring the XMLD effect at the Ni L_2 adsorption edge in a NiO film, local Ni spin direction can be determined and under certain conditions the AFM magnetic domains can also be imaged. Together with the X-ray Magnetic Circular Dichroism (XMCD) effect which determines the FM spin structure, the XMLD effect in NiO films has become a powerful tool for the study of the magnetic exchange interaction in AFM-FM systems [10,11,12]. For example, a spin reorientation of NiO interfacial spins [10] and a creation of a planar AFM domain wall [13] have been observed in NiO/Co system. Zhu *et al.* [14] also proved that the onset of the exchange bias in NiO/$Co_{84}Fe_{16}$ bilayers is accompanied by a preferential repopulation of the NiO AF domains, a key component to the exchange bias.

Despite the great success of the XMLD effect, the determination of the NiO spin structure is not trivial but rather depends on a detailed understanding of the X-ray Linear Dichroism (XLD) spectrum. Generally speaking, the XLD effect should consist of two parts: crystal field effect and magnetic effect. In early studies, the NiO

spin axis was assigned by assuming that the higher energy peak of the Ni L_2 doublet of the XLD spectrum reaches its maximum value when the x-ray polarization vector **E** coincides with the NiO spin axis [7]. However, this assumption was recently revised by Arenholz et. al [15] who showed that this assumption is correct only for the Ni spins parallel to the [100] crystalline direction and that the XMLD effect exhibits a strong anisotropic effect in the NiO $L_{2,3}$ edge. In addition to the complexity of the magnetic contribution to the XLD effect, there also exists crystal field effect to the XLD signal. For example, Haverkort et. al [16] reported that there exists a strong XLD effect for 1ML NiO on Ag(001) at room temperature which is above the Néel temperature and that simultaneously the Ni L_3 absorption peak exhibits a 0.35eV energy shift. The addition of the crystal field effect makes it difficult to isolate the magnetic contribution from the overall XLD effect. Then the interesting question is if we can develop an experimental system in which we eliminate the crystal field effect so that all the XLD effect can be unambiguously identified as the magnetic contribution? In this paper, we report a study of the XLD effect in NiO films grown on vicinal Ag(001) with the steps parallel to the [110] direction. We observe that the atomic steps induce an in-plane magnetic anisotropy and that there exists an in-plane spin reorientation transition from parallel to perpendicular directions of the step edges as the NiO thickness increases above the 3.5nm. The XLD spectrum of the Ni L_3 edge is also carefully studied, and the high temperature measurement result confirms that crystal field effect has no contribution to the XLD effect in this system at the normal incidence of the x-ray.

2. Experiment

A 10-mm diameter Ag(118) single crystal (10° vicinal angle with steps parallel to [110] direction) was used as the substrate. The substrate was mechanically polished down to a 0.25μm diamond-paste finish, followed by a chemical polishing [17], and then further cleaned in an ultrahigh vacuum (UHV) system by cycles of Ar^{+} sputtering at ~1.0 keV and annealing at $600^{o}C$. NiO films were prepared by growing

Ni onto the Ag substrate at 200°C at an oxygen pressure of ~1x10^{-6} Torr. The film quality is further improved by annealing the film at 300°C in the absence of oxygen pressure. The NiO thickness is determined by the Ni deposition rate (~0.5-1.0 Å/min) monitored by a quartz thickness monitor. It was shown that under these conditions NiO forms high quality single crystal film on Ag(001) [18,19]. In order to systematically study the thickness dependent XLD effect, the NiO film was grown into a wedge shape by moving the substrate behind of a mask. The wedge slope is ~1nm/mm with the thickness increasing along the atomic step direction. A thicker NiO film was grown at the end of the wedge for the purpose of registering the NiO wedge.

X-ray absorption spectrum (XAS) measurement was carried out at beamline 4.0.2 of the Advanced Light Source at the Lawrence Berkeley National Laboratory [20] which provides a 99±1% linear polarization of the emitted x-ray. The XAS was measured at different incident angle (θ) and polarization direction (ϕ), as shown in Fig. 1(a), where the incident angle (θ) is defined as the angle between the x-ray incident direction and the sample surface normal direction and the angle ϕ is defined as the angle between the polarization vector and the atomic step direction. The XAS of the Ni^{2+} L edge were recorded at room temperature in the total electron yield mode by measuring the sample current. The high temperature spectrum was collected by measuring the electron yield using an electron channeltron. The thickness-dependent measurement was obtained by laterally moving the sample along the wedge direction with a precision of <0.1mm. The x-ray beam size in the wedge direction is determined by the x-ray entrance slit width (20μm).

3. Result and Discussion

Fig.1(b) shows the thickness dependence of the Ni^{2+} L_3 edge absorption intensity at the normal incident x-ray. It is clearly shown that the intensity increases monotonically with the NiO thickness in the form of $I_{NiO} = I_{NiO}^{\infty}(1-\exp(-d_{NiO}/\lambda_{NiO}))$, where the I_{NiO}^{∞} is the NiO absorption intensity at infinite NiO thickness, and λ_{NiO} is a

phenomenological parameter that reflects the overall effect of the secondary electron escaping distance and the x-ray penetration depth. The fitted value of $\lambda_{NiO} = 5.5 \pm 0.5nm$ is much greater than the secondary electron escape depth of metallic Co and Fe film [21,22].

By measuring the Ni L_2 edge XAS at different x-ray incident angles, we confirmed that the NiO spins prefer to the in the plane direction of the film [7,9]. To determine the spin direction within the film plane, we measured the ϕ-dependence of the XAS at the normal incident of a linearly polarized x-ray [Fig. 1(a)]. XAS spectra for $\vec{E}$//steps (ϕ=0°) and $\vec{E}\perp$steps (ϕ=90°) were taken to identify the existence of the XLD effect. Fig. 2(a-c) shows the representative XAS spectra of the Ni L_2-edge at different NiO thickness. The Ni L_2 XAS spectrum of a NiO film consists of two adsorption peaks and the relative height of these two peaks is usually assumed to be determined by the angle between the x-ray polarization vector $\vec{E}$ and the Ni spin orientation [7,13]. Then the intensity difference of the XAS spectra between ϕ=0° and ϕ=90° in Fig. 2(a-c) clearly exhibits opposite behaviors below and above 3.5nm NiO. For the 2.6nm NiO film, the higher-energy peak at $\vec{E}$//steps (ϕ=0°) is less than that at $\vec{E}\perp$steps (ϕ=90°) and the lower energy peak at $\vec{E}$//steps (ϕ=0°) is greater than that at $\vec{E}\perp$steps (ϕ=90°), but the above behavior of the doublet is obviously reversed for the 4.7nm NiO film. This fact indicates that the Ni spin direction is switched by 90 degrees with increasing the NiO thickness above the critical thickness of 3.5nm where the NiO film doesn't show a difference in the XAS spectra for $\vec{E}$//steps (ϕ=0°) and $\vec{E}\perp$steps (ϕ=90°). It has been shown that the L_2 ratio (R_{L2}) of the XAS spectrum, which is defined as the intensity ratio of the two Ni L_2 peaks (the lower-energy peak divided by the higher-energy peak), describes the angle between the x-ray polarization vector and the Ni^{2+} spin easy axis [7,14]. Fig. 2(d) shows the experimental values of the ϕ-dependent L_2 ratio for the three NiO thicknesses in Fig. 2(a)-(c). While the L_2 ratios of the 2.6nm and 4.7nm NiO films show a sinusoidal ϕ-dependence with

opposite signs, the L_2 ratio of the 3.5nm NiO film shows a constant value at different polarization angles, indicating that the NiO spins of the 3.5nm NiO film don't have a preferred in-plane direction. As the thickness increases from 2.6nm to 4.7nm, we only observe a change in the sign and amplitude of the L_2 ratio with the extremums remaining at $\phi=0^o$ and $\phi=90^o$, showing that the Ni^{2+} spins undergo a 90° easy axis switching at ~3.5nm NiO thickness.

The thickness dependence of the XLD effect is shown in Fig. 3. For NiO thickness less than 1nm, the L_2 ratio is independent of the x-ray polarization angle ϕ, showing an absence of the XLD effect. This is because that the Néel temperature of the NiO film thinner than 1nm is lower than the room temperature. For NiO film thicker than 1nm, the L_2 ratio starts to exhibit a difference between $\phi=0^o$ and $\phi=90^o$, indicating the establishment of an antiferromagnetic order in the NiO film. The XLD value, which is defined as the L_2 ratio difference between $\phi=0^o$ and $\phi=90^o$, increases initially with the NiO thickness with the L_2 ratio at $\vec{E}$ //steps ($\phi=0^o$) greater than at $\vec{E}\perp$steps ($\phi=90^o$), then switches its sign between 3-4nm NiO thickness, and reaches its negative maximum above 4nm NiO thickness. It is worth to note that the above behavior for NiO films grown at 200^oC is different from a previous report on NiO films grown at room temperature [23], which may due to a different structural relaxation of the NiO films at different growth temperature [24]. Since the dependence of the NiO structure on the growth temperature is another topic of research and needs further investigation, we focus only on the XLD analysis on the samples reported in this paper.

In previous studies of the NiO XLD effect, it was usually assumed that the higher-energy peak of the L_2 doublet reaches its *maximum* value (or a *minimum* L_2 ratio) when the x-ray polarization vector is parallel to the Ni^{2+} spin direction. However, all the early measurements were performed for Ni^{2+} spins along [100] crystal axis. Recently, Arenholz et al [15] showed that the XMLD effect actually behaves in an opposite way for Ni^{2+} spins along the [110] crystal axis, i.e., for Ni^{2+} spins parallel to [110] axis the higher-energy peak of the L_2 doublet should reach its

minimum value (or a *maximum* L_2 ratio) when the x-ray polarization vector is parallel to the Ni spin^{2+} direction.. In Fig. 2(e), the L_2 ratio reaches its extremum for x-ray polarization vector parallel to the atomic steps ([110] axis), thus we can at least conclude that the Ni^{2+} spin direction is either parallel or perpendicular to the step [110] direction. Since Ni spin easy axis is parallel to [110] crystal axis, we need to apply the Arenholz's result that the higher-energy peak of the L_2 doublet should reach its *minimum* value (or a *maximum* L_2 ratio) when the x-ray polarization vector is parallel to the Ni^{2+} spin direction. Therefore, we conclude from the result of Fig. 2 and Arenholz's work [15] that the Ni spins in NiO/Ag(118) system is parallel to the steps below 3.5nm NiO and perpendicular to the steps above 3.5nm NiO.

Next we shift our attention to discuss the NiO L_3 peak XLD effect in our NiO/Ag(118) system. As mentioned in the introduction, NiO XLD effect should generally consist of both the magnetic and the crystal field effects. Our previous work shows that the XLD effect of the Ni L_2 peak for NiO films grown vicinal Ag surface with the steps//[110] comes *only* from the magnetic origin for normal incidence of the x-ray [23] because the XLD effect vanishes above the NiO Néel temperature. Therefore the NiO/Ag(118) system can be applied to exam the magnetic and crystal field contributions to the XLD effect of the Ni L_3 peak separately, which is usually difficult to achieve in other single crystalline NiO systems where both magnetic and crystal field effects are present at the same time. Fig.4 (a) and (b) show the XAS spectra measured on NiO films of 2nm (Ni^{2+} spin parallel to the steps) and 6nm (Ni^{2+} spin perpendicular to the steps) thicknesses. We first exam the crystal field effect by measuring the XAS spectra at a 60 degree incident angle [Fig. 1(a)] and two polarization directions. First, we observed a strong XLD effect at 60 degree incident angle. Second, the L_3 peak exhibits an energy shift towards higher energy for ϕ changes from 90° to 0°. Although the amount of this energy shift (ΔE) decreases with the NiO thickness (ΔE ~200meV for 2nm NiO film and ΔE ~80meV for 6nm NiO film), the L_3 peak shifts its energy in the same direction for both 2nm and 6nm NiO films regardless of their spin direction difference. The above result shows that the XLD effect, especially the L_3 peak energy shift, in NiO/Ag(118) at 60

degree x-ray incident angle is mainly contributed from the crystal field effect, in agreement with the previous report [16]. At the normal incidence ($\theta = 0^0$) the L_3 XAS shows a minimal XLD effect as compared to the $\theta = 60^0$ case, however a tiny energy shift ($\Delta E = 18 \pm 2meV$) of the L_3 peak is still detectable as shown in the inset of Fig. 4. Since this tiny energy shift is comparable to the energy reproducibility of the beamline, to reduce the uncertainty of the energy peak positions at the two polarizations, we measured the XAS spectra by alternating the polarization at each energy of the XAS measurement. In this way, the spectra with two polarizations have exact same energy at each energy step of the measurement so that the error bar of the energy shift between the two polarizations can be minimized. The NiO L_3 peak shows a lower energy at ϕ=0° than at ϕ=90° for 2nm NiO (see inset of Fig. 4a) and a higher energy at ϕ=0° than at ϕ=90° for 6nm NiO (see inset of Fig. 4b). Recalling that the NiO exhibits an in-plane SRT at 3.5nm thickness, then the above result reflects the fact that at normal x-ray incidence the XLD is mainly contributed from the magnetic effect. Since the Ni^{2+} spins were determined to be parallel to the steps at 2nm, and perpendicular to the steps at 6nm, we conclude that the NiO L_3 peak exhibits a higher energy for the x-ray polarization perpendicular to the spin direction. Fig. 4(c) and (d) show the detailed XLD spectra (the difference of the XAS spectra at ϕ=0° and at ϕ=90°) at the normal incidence of the x-ray for the 2 nm and 6nm NiO films. Indeed these two XLD spectra show a great similarity except the opposite signs (spectrum of Fig. 4c is plotted after reversing its sign in Fig. 4d for comparison). The smaller amplitude of the 2nm film spectrum is due to the fact that the Néel temperature of the 2nm NiO is closer to room temperature than the 6nm film. It is also worth to note that the XLD spectra we obtained on NiO film is similar to the spectra in the $NiFe_2O_4$ and Co/NiO(001) systems [15].

To further confirm that the XLD effect of the NiO L_3 edge is completely from the magnetic effect at the normal incidence of the x-ray, we performed high temperature measurement on our samples. The XLD effect of the 4.3nm NiO film at the normal incidence of the x-ray at room temperature disappears at 570K which is above the

bulk NiO Néel temperature (523K). The above observation fully proves that the XLD effect at the NiO L_3 edge at $\theta=0^0$ comes completely from the magnetic effect. In contrast, the similarity of the two XLD spectra at room temperature and at 570K for the $\theta=60^0$ case shows that the XLD effect in this case comes mainly from the crystal field effect.

In summary, we find that there exists an in-plane spin reorientation transition of for NiO films grown on Ag(118) surface at 200°C. The Ni spin direction is parallel to the step direction for NiO films thinner than 3.5nm, and perpendicular to the steps for the films thicker than 3.5m. At the normal incidence of the x-ray, we proved that the XLD effect at the Ni L_3 edge comes completely from the magnetic effect, and the XAS spectra for x-ray polarization being parallel and perpendicular to the steps exhibit a tiny energy shift ($\Delta E = 18 \pm 2meV$).

Acknowledgement

This work was supported by National Science Foundation DMR-0405259 and U.S. Department of Energy DE-AC03-76SF00098, the National Natural Science Foundation of China, 973-project under Grant No. 2006CB921303, Shanghai Science and Technology Committee, and Shanghai Education Development Foundation.

The Advanced Light Source is supported by the Director, Office of Science, Office of Basic Energy Sciences, of the U.S. Department of Energy under Contract No. DE-AC02-05CH11231.

Figures:

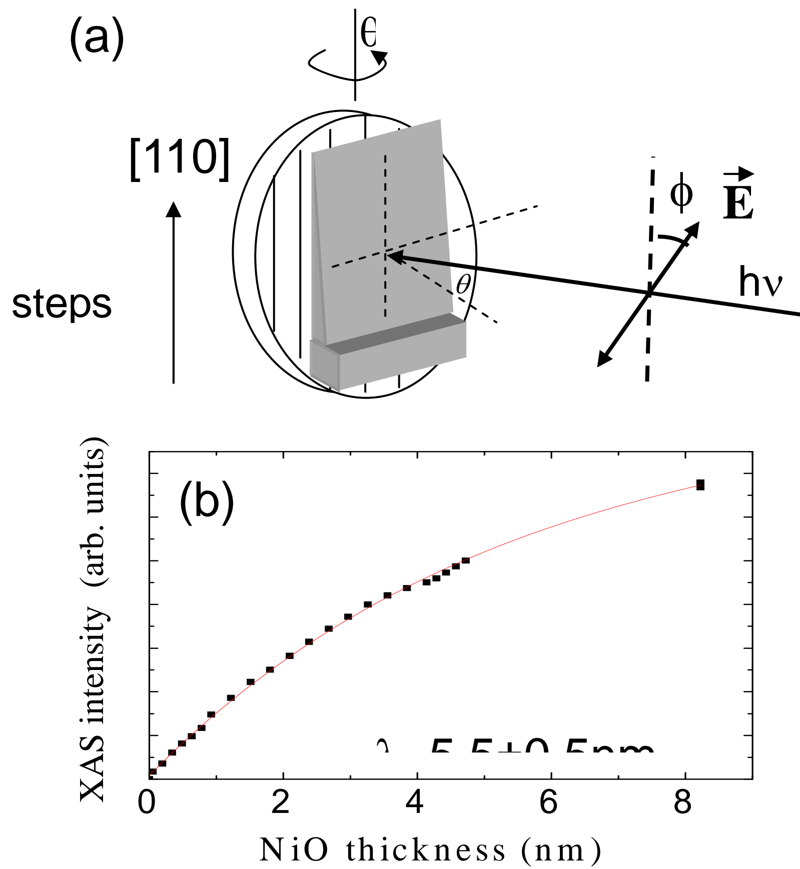

Fig. 1: (a) Schematic drawing of the experimental geometry. (b) XAS intensity of the Ni L_3 peak at normal incidence of the x-ray as a function of the NiO thickness. The solid line represents the fitting result (see text).

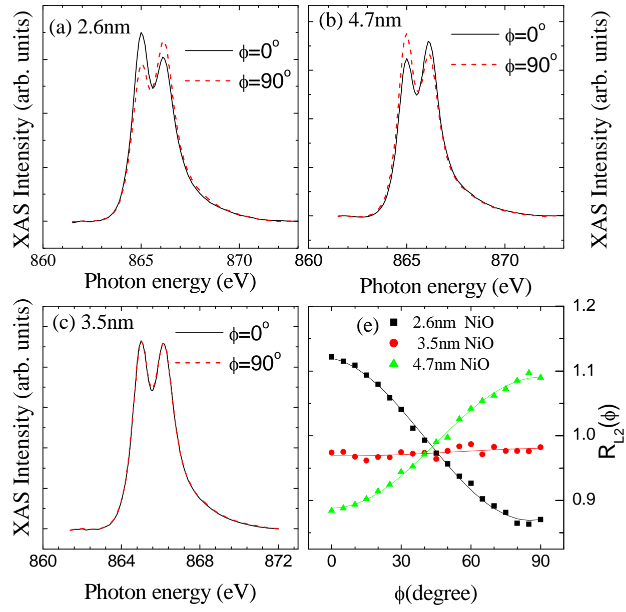

Fig. 2: Ni L_2 edge XAS spectra of NiO films grown on Ag(118) at normal incidence of the x-rays ($\theta = 0^0$) at NiO thickness of (a) 2.6nm, (b) 4.7nm, and (c)3.5nm. (d) Ni L_2 ratio as a function of polarization angle ϕ for the NiO films in (a)-(c).

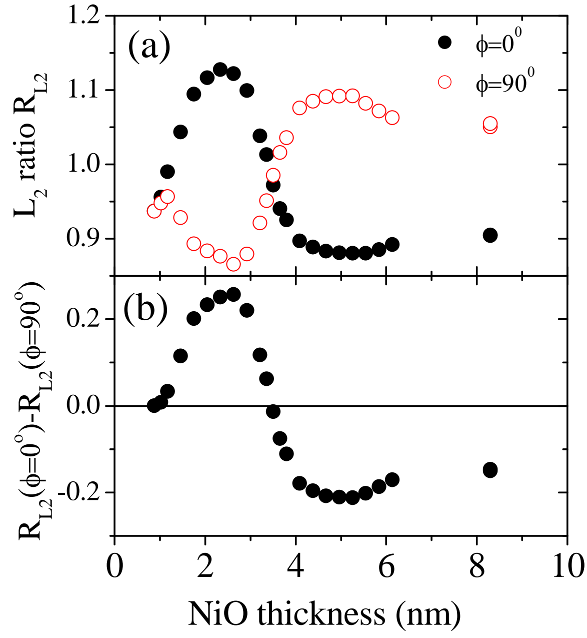

Fig.3: (a) Thickness-dependent L_2 ratio at the normal incidence of the x-rays ($\theta = 0^o$) for the x-ray polarization parallel ($\phi = 0^0$) and perpendicular ($\phi = 90^0$) to the atomic steps. (b) L_2 ratio difference between $\phi = 0^0$ and $\phi = 90^0$ as a function of the NiO thickness.

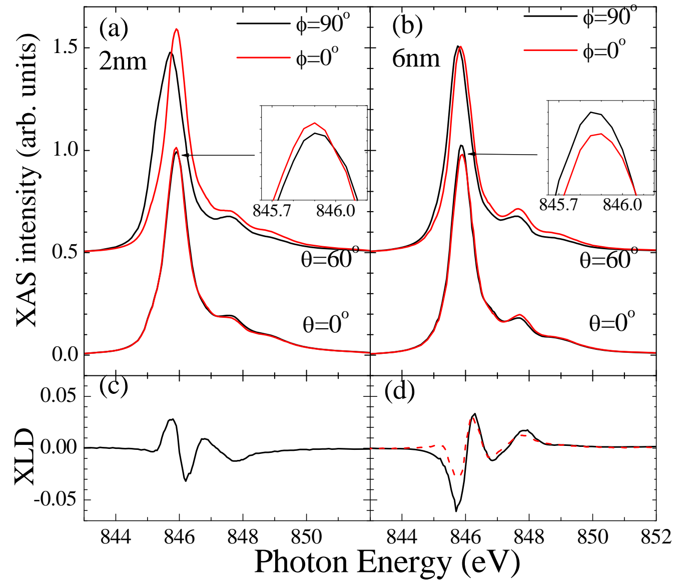

Fig. 4: L_3 edge NiO XAS spectra at different incident angles and polarization directions for NiO grown on Ag(118) with the thickness of (a) 2nm and (b) 6nm. The insets are the zoom-in L_3 peak at the normal incidence of the x-rays. (c) and (d) are the XLD spectra of 2nm and 6nm thick NiO films at the normal incidence of the x-rays. The dashed line of XLD spectrum in (d) is the spectrum of (c) after reversing its sign.

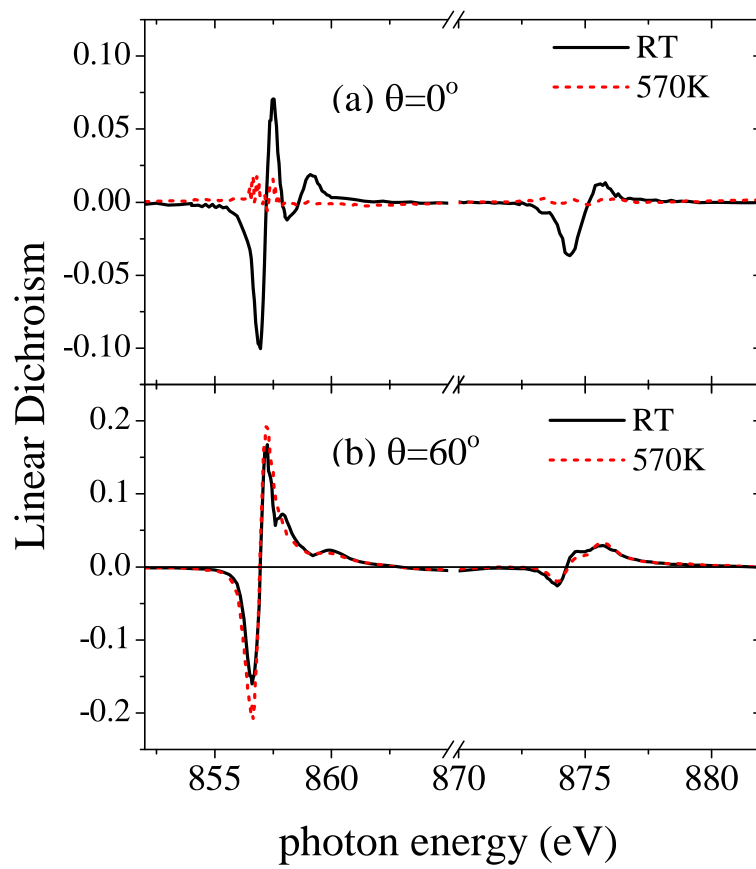

Fig. 5: XLD spectra of 4.3nm NiO film measured at room temperature and 570K at different incident angles of the x-ray: (a) $\theta = 0^0$ and (b) $\theta = 60^0$.

1 W. H. Meiklejohn and C. P. Bean, Phys. Rev. **102**, 1413 (1956).

2 J. Nogués and Ivan K. Schuller, J. of Magn. Mag. Mat. **192**, 203 (1999).

3 R L Stamps, J. Phys. D: Appl. Phys. **33**, R247 (2000).

4 Miguel Kiwi, J. of Magn. Mag. Mat. **234**, 584 (2001).

5. B. T. Thole, G. van der Laan, and G. A. Sawatzky, Phys. Rev. Lett. **55**, 2086 (1985).

6. Pieter Kuiper, Barry G. Searle, Petra Rudolf, L. H. Tjeng, and C. T. Chen, Phys. Rev. Lett. **70**, 1549 (1993).

7 D. Alders, L. H. Tjeng, F. C. Voogt, T. Hibma, G. A. Sawatzky, C. T. Chen, J. Vogel, M. Sacchi, and S. Iacobucci, Phys. Rev. B **57**, 11623 (1998).

8 G. van der Laan, Phys. Rev. Lett. **82**, 640 (1999).

9 J. Stöhr, A. Scholl, T. J. Regan, S. Anders, J. Lüning, M. R. Scheinfein, H. A. Padmore, and R. L. White, Phys. Rev. Lett. **83**, 1862 (1999).

10 H. Ohldag, A. Scholl, F. Nolting, S. Anders, F. U. Hillebrecht, and J. Stöhr, Phys. Rev. Lett. **86**, 2878 (2001).

11 H. Ohldag, T. J. Regan, J. Stöhr, A. Scholl, F. Nolting, J. Luning, C. Stamm, S. Anders, R. L. White, Phys. Rev. Lett. **87**, 247201 (2001).

12 F. Nolting, A. Scholl, J. Stöhr, J. W. Seo, J. Fompeyrine, H. Siegwart, J.-P. Locquet, S. Anders, J. Lüning, E. E. Fullerton, M. F. Toney, M. R. Scheinfein, H. A. Padmore., Nature (London) **405**, 767 (2000).

13 A. Scholl, M. Liberati, E. Arenholz, H. Ohldag, and J. Stöhr, Phys. Rev. Lett. **92**, 247201 (2004)

14 W. Zhu, L. Seve, R. Sears, B. Sinkovic, and S. S. P. Parkin, Phys. Rev. Lett. **86**, 5389 (2001).

15 Elke Arenholz, Gerrit van der Laan, Rajesh V. Chopdekar, and Yuri Suzuki, Phys. Rev. Lett. **98**, 197201 (2007).

16 M. W. Haverkort, S. I. Csiszar, Z. Hu, S. Altieri, A. Tanaka, H. H. Hsieh, H.-J. Lin, C. T. Chen, T. Hibma, and L. H. Tjeng, Phys. Rev. B **69**, 020408 (2004).

17. N. Q. Lam, S. J. Rothman, and L. J. Nowicki, J. Electro-Chem. Soc. **119**, 715 (1972).

18. C. Giovanardi, A. di Bona, and S. Valeri, Phys. Rev. B **69**, 075418 (2004).

19. C. Lamberti, E. Groppo, C. Prestipino, S. Casassa, A. M. Ferrari, C. Pisani, C. Giovanardi, P. Luches, S. Valeri, and F. Boscherini, Phys. Rev. Lett. **91**, 046101 (2003).

20. A. T. Young, E. Arenholz, S. Marks, R. Schlueter, C. Steier, H. A. Padmore, A. Hitchcock, and D. G. Castner, J. Synchtrotron Radiation **9**, 270 (2002).

21 Y. Z. Wu, C. Won, A. Scholl, A. Doran, F. Toyoma, X. F. Jin, N. V. Smith, and Z. Q. Qiu, Phys. Rev. B **65**, 214417 (2002).

22 R. Nakajima, J. Stöhr, and Y. U. Idzerda, Phys. Rev. B **59**, 6421(1999).

23 Y. Z. Wu,Z. Q. Qiu,Y. Zhao, A. T. Young, E. Arenholz, and B. Sinkovic, Phys. Rev. B **74**, 212402 (2006).

24 C. Giovanardi, A. di Bona, S. Altieri, P. Luches, M. Liberati, F. Rossi, S. Valeri, Thin Solid Films **428**,195 (2003).